J Low Temp Phys (2014) 176:841–847
DOI 10.1007/s10909-013-1068-2

Optical Measurements of SuperSpec: A Millimeter-Wave On-Chip Spectrometer

S. Hailey-Dunsheath · P. S. Barry · C. M. Bradford · G. Chattopadhyay · P. Day · S. Doyle · M. Hollister · A. Kovacs · H. G. LeDuc · N. Llombart · P. Mauskopf · C. McKenney · R. Monroe · H. T. Nguyen · R. O'Brient · S. Padin · T. Reck · E. Shirokoff · L. Swenson · C. E. Tucker · J. Zmuidzinas

Received: 6 September 2013 / Accepted: 23 December 2013 / Published online: 23 January 2014

Abstract SuperSpec is a novel on-chip spectrometer we are developing for (sub)millimeter wavelength astronomy. Our approach utilizes a filterbank of moderate resolution ($R \sim 500$) channels, coupled to lumped element kinetic inductance detectors (KIDs), all integrated onto a single silicon chip. The channels are half-wave resonators formed by lithographically depositing segments of superconducting transmission line, and the KIDs are titanium nitride resonators. Here we present optical measurements of a first generation prototype, operating in the 180–280 GHz frequency range. We have used a coherent source to measure the spectral profiles of 17 channels, which achieve linewidths corresponding to quality factors as high as $Q_{\mathrm{filt}} = 700$, consistent with

S. Hailey-Dunsheath (✉) · M. Hollister · A. Kovacs · C. McKenney · R. O'Brient · S. Padin · E. Shirokoff · L. Swenson · J. Zmuidzinas
California Institute of Technology, Mail Code 301-17, 1200 E. California Blvd., Pasadena, CA 91125, USA
e-mail: haileyds@caltech.edu

P. S. Barry · S. Doyle · C. E. Tucker
School of Physics & Astronomy, Cardiff University, 5 The Parade, Cardiff CF24 3AA, UK

C. M. Bradford · G. Chattopadhyay · P. Day · H. G. LeDuc · R. Monroe · H. T. Nguyen · T. Reck
Jet Propulsion Laboratory, 4800 Oak Grove Drive, Pasadena, CA 91109, USA

A. Kovacs
Institute for Astrophysics, University of Minnesota, 116 Church St SE, Minneapolis, MN 55455, USA

N. Llombart
Optics Department of the Complutense University of Madrid, C. Arcos de Jalon No. 118, 28037 Madrid, Spain

P. Mauskopf
Arizona State University, 650 E. Tyler Mall, Tempe, AZ 85287, USA

the designed values plus additional dissipation characterized by $Q_i \approx 1440$. We have also used a Fourier Transform Spectrometer to characterize the spectral purity of all 72 channels on the chip, and measure typical out of band responses ∼30 dB below the peak response.

Keywords Kinetic inductance detector · Millimeter-wave · Spectroscopy

1 Introduction

The epoch of reionization and the birth and subsequent growth of galaxies in the first half of the Universe's history ($z \gtrsim 1$) are key topics in modern astrophysics. Measurements of the cosmic far-IR background indicate that in aggregate, much if not most of the energy released by stars and accreting black holes over cosmic time has been absorbed and reradiated by dust [3]. A complete understanding of galaxy evolution since reionization therefore requires observations at (sub)millimeter wavelengths, where the dust emission peaks, and the extinction of diagnostic spectral lines is minimized. Survey spectroscopy at (sub)millimeter wavelengths, using a multi-beam spectrometer such as we describe here, is uniquely poised to access the high-redshift Universe, both through the measurement of individual galaxies, and via statistical studies in wide-field tomography. In particular, the 158 μm [CII] transition is typically the brightest spectral feature in dusty galaxies, and promises to be a powerful probe of galaxies at redshifts $z \geq 3$, where it is shifted into the telluric windows at $\lambda \geq 600$ μm [7].

SuperSpec is a novel, ultra-compact spectrometer-on-a-chip for (sub)millimeter wavelength astronomy. Its very small size, wide spectral bandwidth, and highly multiplexed detector readout will enable construction of powerful multi-beam spectrometers for high-redshift observations. We are currently developing this technology with $R \sim 500$ spectrometers covering the 190–310 GHz band, with the aim of deploying a future wide-band survey spectrometer for the 25 m CCAT telescope, with tens of thousands of detectors employed in tens of beams covering the 190–520 GHz band. The proposed instrument will be optimized for measuring the bright atomic fine-structure and molecular rotational lines from interstellar gas in galaxies, and particularly for [CII] observations at $z \approx 3$–9. This same technology will also be deployed in the proposed TIME, a statistical survey instrument designed to tomographically map out the [CII] line during reionization (see Stanizewski proceedings).

2 First Generation Prototype

Free space radiation is coupled into a transmission line (the feedline) on our prototype chips using a direct-drilled, multiple-flare angle feed horn [1]. The circular waveguide output of the horn is converted to a single mode oval waveguide and fed with a planar probe, fabricated from the 25 μm thick device layer of a SOI wafer that forms the spectrometer chip (T. Reck, in prep). The probe couples through a CPW transition segment to the impedance-matched microstrip that forms the feedline. Simulations of this design show a coupling efficiency above 90 % from 190 to 310 GHz.

SuperSpec employs a filterbank architecture [1,4,6]. Incoming radiation propagates down the feedline past a series of tuned resonant filters, each of which consists of a section of transmission line of length $\lambda_i/2$, where λ_i is the resonant wavelength of channel i. These half-wave resonators are coupled to the feedline and to power detectors with adjustable coupling strengths (described by quality factors $Q_{\rm feed}$ and $Q_{\rm det}$, respectively) that determine the net filter quality factor $Q_{\rm filt}$, which is equal to the spectrometer resolving power R. The transmission line for both the feedline and the resonator is microstrip, consisting of superconducting Nb traces on a Si substrate beneath an amorphous silicon-nitride (Si_3N_x) dielectric and Nb ground plane. The signal power admitted by each resonator is dissipated in a segment of lossy meander formed from titanium nitride (TiN). Radiation at frequencies above the superconducting gap in the TiN film ($f \sim 147$ GHz for $T_c \sim 2$ K) breaks Cooper pairs and generates quasiparticles, resulting in a perturbation of the complex impedance.

The TiN meander is connected in parallel to an interdigitated capacitor (IDC) made from the same TiN material to form a lumped element kinetic inductance detector (KID) [6]. Perturbations to the complex impedance of the meander translate into changes in the dissipation and resonant frequency of the KIDs, which operate with resonant frequencies in the 100–200 MHz range. Each KID is coupled to a coplanar waveguide readout feedline (CPW) by a small coupling capacitor, formed by TiN on the KID side, and Nb on the readout side. The chip is cooled by a ^{3}He sorption refrigerator to 220 mK, which is sufficiently below the TiN T_c to keep the thermal quasipartical density below that of the optically-generated quasiparticles, while also as high as possible to minimize two-level system (TLS) noise.

We have fabricated and characterized a first generation prototype SuperSpec test device. This device includes three types of mm-wave features: 73 tuned mm-wave filters, 4 in-line broad-band detectors interspersed over the full length of the feedline, and a terminating absorber. The 73 tuned filters span the 180–280 GHz range, and have design values of $Q_{\rm feed}$ and $Q_{\rm det}$ targeting (with no additional dissipation) $Q_{\rm filt,design} =$ 300–1400. This range of $Q_{\rm filt,design}$ is intended to test our ability to tune the channel quality factor in the vicinity of $R \sim 500$. The in-line broad-band detectors consist of a short ($<\lambda_{\rm min}/4$) feedline meander in close proximity to a TiN absorber similar to that used in the tuned filters. The proximity coupling between the feedline and the absorber is designed for an approximately flat 0.5 % absorption across the full mm band, which produces an optical loading comparable to that in the spectrometer channels. The terminating absorber consists of a length of meandered feedline surrounded by TiN meander, and is designed to absorb any power arriving at the end of the feed (reducing reflections to $<$20 dB). Four long segments of the terminating absorber are used as the inductors for an additional set of broad-band absorber KIDs.

2.1 Coherent Source Measurements

We have characterized a subset of our channels using a local oscillator (LO) chain, which provides a $\times 15$ frequency multiplication of a microwave tone. The LO is coupled to a feed horn, and radiates directly into the cryostat. The source can be tuned to cover the 180–280 GHz range, and frequency sweeps across our band are used to measure the line profiles of individual channels. For the measurements presented here

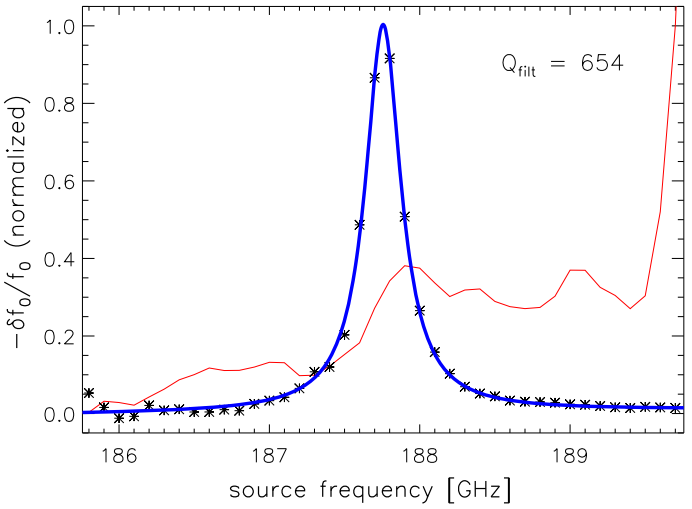

Fig. 1 Spectral profile of a high-Q ($Q_{\rm filt} = 654$) channel measured with a swept coherent source (*black points*) and a Lorentzian fit (*thick blue line*). Data points show the measured response normalized by the response of a broad-band KID (*thin red line*) (Color figure online)

we place a low-pass optical filter with cutoff at 210 GHz in the beam, in order to reject contamination from harmonics in the LO chain. This setup allows characterization of the 17 lowest frequency channels, with $f_0 = 184$–210 GHz, and $Q_{\rm filt,design} = 300$–$1400$. We note that two low-pass optical filters at 300 and 330 GHz inside the cryostat prevent excitation of the harmonics of the spectrometer resonators. The LO source is amplitude-modulated at 2 Hz, fast enough to avoid any excess low-frequency system noise. The KID is read out using a standard homodyne detection scheme, and we toggle the readout between a channel and a nearby broadband in-line KID used to normalize the channel response.

In Fig. 1 we show the peak-normalized profile of a representative high-Q channel. The fractional frequency response $\delta x = \delta f_0/f_0$ of the KID normalized by the peak value is:

$$\frac{-\delta x(f)}{(-\delta x)_{\rm max}} = \frac{1}{1 + 4Q_{\rm filt}^2\left(\frac{f-f_0}{f_0}\right)^2}, \tag{1}$$

where f_0 is the resonant frequency, and $Q_{\rm filt}$ is the filter quality factor. The filter quality factor is given by:

$$1/Q_{\rm filt} = 1/Q_{\rm det} + 1/Q_{\rm feed} + 1/Q_i, \tag{2}$$

where $Q_{\rm i}$ is the internal quality factor accounting for dissipative loss in the resonator [1]. In general, the line profiles are well characterized by Eq. 1, and fitting to this function allows an estimate of $Q_{\rm filt}$ for each channel. We measure filter quality factors as high as $Q_{\rm filt} = 700$, and this provides a conservative lower limit on the dissipative quality factor Q_i. An improved estimate of Q_i may be obtained by comparing

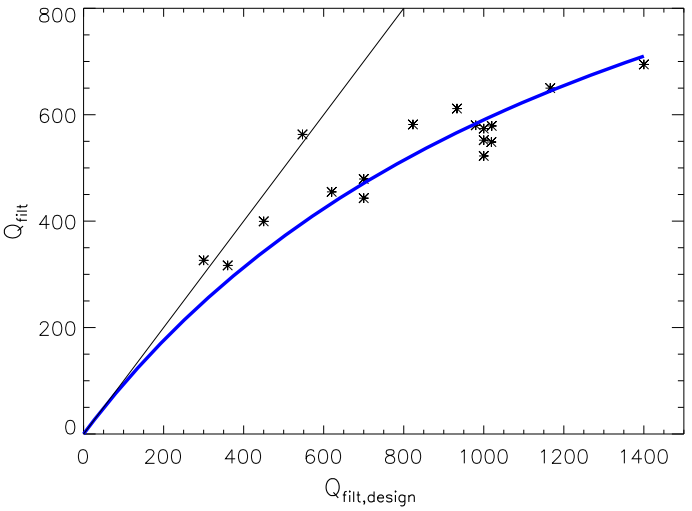

Fig. 2 Comparison of the measured and designed linewidths for the 17 channels at $f_0 = 184$–210 GHz and $Q_{filt,design} = 300$–1400 (see text). Some of the points with $Q_{filt,design} = 1000$ have a small horizontal offset for clarity. *Thin black line* is drawn for $Q_{filt} = Q_{filt,design}$, *thick blue line* shows $Q_{filt}^{-1} = Q_{filt,design}^{-1} + Q_i^{-1}$ for $Q_i = 1440$ (Color figure online)

the measured Q_{filt} with the designed loss-less quality factor, assuming the targeted values of Q_{det} and Q_{feed}. This assumption is supported by the fact that we achieve the designed quality factor for $Q_{filt} < 400$, where dissipative loss is negligible (Fig. 2). A fit to the set of all measured channels using Eq. 2 yields a best fit value of $Q_i = 1440$ (Fig. 2).

The dominant source of dissipation in the resonator is expected to be the silicon-nitride dielectric layer in the microstrip. The loss tangent inferred from our estimated Q_i is $\tan\delta = 1/Q_i = 7 \times 10^{-4}$. This value falls between published measurements of silicon–nitride at $f = 6$ GHz ($\tan\delta \approx 10^{-4}$) [5] and $f \approx 1.5$ THz ($\tan\delta \approx 5 \times 10^{-3}$) [2]. To operate efficiently as an astronomical spectrometer the dissipative losses must be sufficiently small to allow high detection efficiency with moderate resolving power. For a matched resonator ($Q_{feed} = Q_{det}$) the fraction of power on the feedline terminating in the detector on resonance is:

$$\eta_{filt} = \frac{1}{2}\left[1 - \frac{Q_{filt}}{Q_i}\right]^2. \tag{3}$$

With no losses the filter efficiency is $\eta_{filt} = 50$ %, and with $Q_i = 1440$ this drops by less than a factor of 2 for $Q_{filt} \leq 420$.

2.2 Fourier Transform Spectroscopy

We have obtained full band spectra for all channels using a Martin–Puplett Interferometer, with 293 and 78 K blackbodies at the input ports. The 73 spectrometer

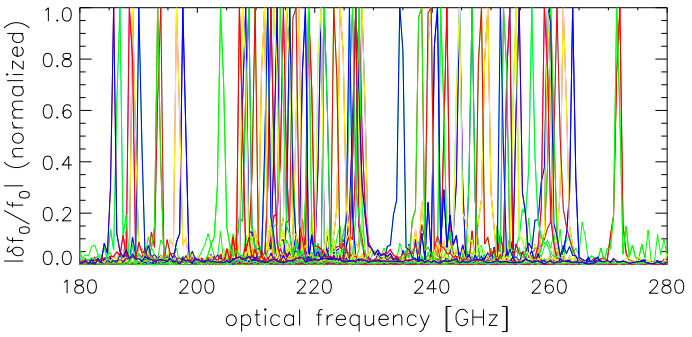

Fig. 3 Full set of 72 channel profiles, measured simultaneously with an FTS and CASPER-ROACH based FPGA multitone readout. Each color is a separate channel. Non-uniform sampling of frequency space is in part by design, and also reflects scatter between designed and measured f_0. Noise from 272 GHz channel produces features at 0.05–0.1 (*green*) (Color figure online)

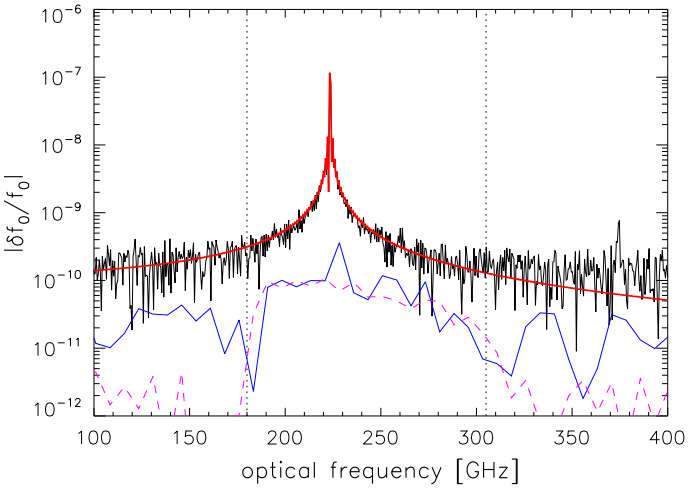

Fig. 4 FTS measurement of the spectral profile of a typical channel (*thin black*). Overplotted are a Lorentzian profile fit (*thin red*), the residuals binned (*thin blue*), the scaled profile of the first terminator (*dashed magenta*), and the expected bandpass defined by feed horn, waveguide probe, and metal-mesh filters (*dotted black vertical lines*). Outside of the narrow channel profile, the response is ∼0.1 % the peak value for most channels, and closely matches the profile measured on the terminator (Color figure online)

channels and 8 broadband KIDS were read out in parallel using a CASPER-ROACH based FPGA readout system. The fourier transform spectrometer (FTS) provides an unapodized spectral resolution of ≈0.6 GHz, compared with the 0.3–0.9 GHz width of the spectrometer channels. Compared with the LO measurements, the FTS measurements do not cleanly resolve the channel profiles, but they do provide a smooth spectral signal that better enables a characterization of the broad-band channel response. In Fig. 3 we show the normalized spectra of all functioning (72/73) channels.

In Fig. 4 we show the response of a representative channel, along with that of the first terminator. We fit models directly to the interferograms, and in general find that

all channel profiles are well described by narrow Lorentzians. The residuals show a detectable broad-band response with the same spectral profile as that of the terminators and inline broad-band KIDs. This indicates a finite amount of direct coupling between the feed line and the channel KIDs that bypasses the half-wave resonators. For typical channels the broad-band response is $\sim 0.1\,\%$ of the peak in-band response.

Acknowledgments This project is supported by NASA Astrophysics Research and Analysis (APRA) Grant No. 399131.02.06.03.43. ES, CMM, and LJS acknowledge support from the W. M. Keck Institute for Space Studies. MIH, LJS, and TR acknowledge support from the NASA Postdoctoral Program. PSB acknowledges the continuing support from the Science and Technology Facilities Council Ph.D studentship programme and grant programmes ST/G002711/1 and ST/J001449/1. Device fabrication was performed the JPL Microdevices Laboratory.

References

1. P.S. Barry et al., in *Society of Photo-Optical Instrumentation Engineers (SPIE) Conference Series*, vol. 8452 (SPIE, Bellingham, WA, 2012)
2. G. Cataldo, J.A. Beall, H.-M. Cho, B. McAndrew, M.D. Niemack, E.J. Wollack, Opt. Lett. **37**, 4200 (2012)
3. D.J. Fixsen, E. Dwek, J.C. Mather, C.L. Bennett, R.A. Shafer, ApJ **508**, 123 (1998)
4. A. Kovács et al., in *Society of Photo-Optical Instrumentation Engineers (SPIE) Conference Series*, vol. 8452 (SPIE, Bellingham, WA, 2012)
5. A.D. O'Connell et al., Appl. Phys. Lett. **92**, 112903 (2008)
6. E. Shirokoff et al., in *Society of Photo-Optical Instrumentation Engineers (SPIE) Conference Series*, vol. 8452 (SPIE, Bellingham, WA, 2012)
7. R. Wang et al., ApJ **773**, 44 (2013)